Article

Low Power FPGA Implementation of a Smart Building Free Space Optical Communication System

Rehab Ali [1], Hossameldin Eassa [2], Hesham H. Aly [1], Mohamed Abaza [1,*] and Saleh M. Eisa [1]

1   Electronics and Communication Engineering Department, Arab Academy for Science, Technology and Maritime Transport, Giza P.O. Box 2033, Egypt; rehab_ali@aast.edu (R.A.); hesham_aly@aast.edu (H.H.A.); saleheisa@aast.edu (S.M.E.)
2   Electronics and Communication Engineering Department, Arab Academy for Science, Technology, and Maritime Transport, Cairo P.O. Box 12577, Egypt; hossam_al-din_easa@student.aast.edu
*   Correspondence: Mohamed.abaza@aast.edu

Abstract: Free Space Optical (FSO) communication systems have extensively invaded the speed of smart city evolution due to the current surge in demand for wireless communication spots that can match recent challenges due to high technical leaps in smart city evolution. As the number of users is vastly increasing throughout all networks in the form of machines, devices, and variously distinct objects, FSO is a hugely recommended robust communication system that mitigates a lot of RF disadvantages on the field with no need for licensing, fast rollout time, and low cost. This paper shows an exploit of a Low Power Field Programmable Gate Array (FPGA) based FSO communication system designed for Line of Sight (LOS) Building to Building Communication over a distance of 12 m using a 650 nm Visible Light (VL) red laser source via On-Off Keying (OOK) and higher-level Intensity Modulation (IM)/Pulse Width Modulation (PWM) schemes. The implemented system reached a doubled data rate than OOK of 230 kbps using the IM technique. Traffic monitoring and building security status can be frequently updated between adherent buildings, each scanning its zone real-time conditions and sharing them with the neighboring links.

1. Introduction

The development of Information and Communication Technologies (ICT) during the last few decades has sparked a trend of imbuing everyday items with intelligence to make modern life easier. As a consequence of the goal of developing a technologically luxurious future, the Smart Cities vision emerges. The Smart City (SC) paradigm was created as a consequence of multiple and different kinds of motivations, such as the urbanization prominence that an increasing number of cities are initiating through new SC models nowadays [1]. The eagerness behind the conceptualization of improving the qualities of citizens' modern lives and technologizing even day-to-day basic activities was a newly found golden aspect towards a smarter world [2].

The most recent highlight SC infrastructures have established is Intelligent Buildings (IB). The IB concept can be viewed from a multi-industrial perspective, involving the perfect balance of automation, energy, structure, services, and building maintenance to increase comfort and adapt to social stimulation [3].

State-of-the-art communication techniques between IBs are highly recommended to be implemented using Free Space Optics (FSO) as it possesses huge flexibility options for the currently evolving IoT exploitations and has the potential to support large device inquiries and resource management in the clouding era [1]. Hybrid communication systems are usually deployed using integrated FSO and optical fiber technologies in a combined infrastructure that forms an optimum communication track between different nodes [4].

Successful low-cost and versatile wireless communication between neighboring buildings can be developed for sharing each building's security recognition and zone conditions on a frequent monitoring basis.

To begin with, optical wireless communications have set up different platforms and territories for placing successful communication spots. Data from Ref. [5] emboldens the classifications of optical wireless technologies, as shown in Figure 1.
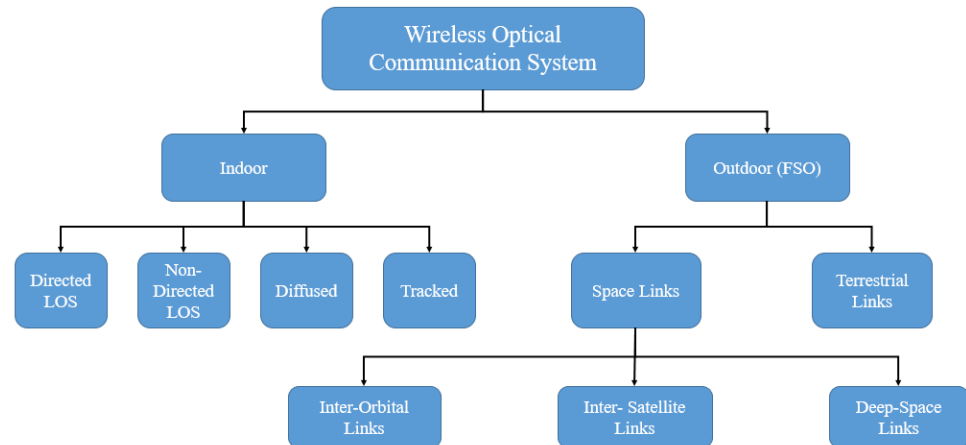

Figure 1. Wireless Optical Communications Classifications. Data from Ref. [5].

For outdoor FSO links applications, there are two types of networks: space links and terrestrial links. The primary motivation for establishing such a network is to provide global internet coverage, i.e., the ability to communicate between any two points on Earth, particularly in areas where terrestrial internet is scarce or nonexistent. One of the pioneering technologies in satellite communications is StarLink which is described as a huge low earth orbit (LEO) constellation created by SpaceX for providing global coverage, high bandwidth, and low latency satellites [6,7].

For smart building communications, a line of sight (LOS) FSO link between buildings is the item of recognition and the main focus of this research. In recent years, there has been an extremely competitive aspect between conventional wireless communication such as radio frequency (RF) and the newly intriguing alternative technologies involving utilizing signals in an optical form [8]. Among the candidate innovations these technologies offer is the FSO communication system, where a signal is transferred from an electrical to an optical one and carried through a free space medium in the form of a visible light (VL) beam or an infrared (IR) beam. The fact that FSO eliminates most of the cons of RF communication makes it a strong opponent technique nowadays [4,5].

The presence of linked sensors or devices in the city is required for these applications, giving the green light for new alternative linkages to step in. Mobile and network operators must adjust their strategies in this scenario to keep up with the city's technological advancements and the conquering of other strategies and infrastructures [9]. FSO technology displays various advantages such as non-necessity of a licensed bandwidth, high security of data and negligibility of interference and jamming occurrence, higher data rates, and cheaper rollout cost. With these advantages come some challenging situations an FSO network can encounter, including weather turnovers such as rain and foggy space, atmospheric turbulence, scintillation, scattering, etc. [10]. Table 1 shows a detailed comparison between RF conventional wireless technology and optical wireless communications with a distinction of the bandwidth variety between RF bands and OWC bands.

Table 1. RF vs. OWC technologies [5,11,12].

Metric of Concern	Conventional Wireless Technology (RF)	Optical Wireless Communications (OWC)
Signal Type	RF or Microwave Electromagnetic waves in free space	Light modulated signals through free space
Cost	Expensive Infrastructure	Low-cost Implementation
Noise	Interference and Jamming Threats	Ambient Light
Bandwidth	Limited Bandwidth according to the operating bands (VHF = 30–300 MHz) (UHF = 300–3000 MHz) (SHF = 3–30 GHz)	The accessible OW spectral areas, such as 1 mm–750 nm for infrared, 780 nm–380 nm for visible light, and 10 nm–400 nm for UV, provide infinite bandwidth.
License	Need for Licensing	No need for Licensing
Data Rates	Less than 2 Gbps	Up to 10 Gbps
Distance	Up to 80 km	2~8 km (FSO)

FSO systems have a vast range of applications, such as outdoor wireless networks, LAN segmental small networks, optical fiber connections backup networks, backhauling, and military communications [13]. Unlike fiber-optical installations that despite being one of the most reliable networks have the most expensive cost, FSO is a much simpler network that requires only two optical transceivers for a full-duplex link, with the proper choice of optical source used to transmit the signal [14].

With the optimum kind of modulation depending on data rate needs and the type of territory the system is installed in, a fully-functioning low-cost communication spot is obtained [9,10,15,16]. Apart from the competitive side, RF communications happen to require complementary FSO transceiver links that can reinforce the quality of service for remotely located users and increase the overall network capacity. Another example of outdoor FSO links is presented in [17]. To eliminate the direct LOS drawback of alignment and setup angle immobility problems multi-FSO transceivers can be tiled up to ensure the maximum spatial expansion and optimized performance for outdoor FSO links.

Designing a high-rate and resource-efficient network infrastructure for 5G and beyond has received a lot of interest and turned into an extremely viral research topic. Another hybrid example is represented in [18], where Coexisting RF networks are integrated with optical-fiber networks and OWC systems to create an ultra-high coverage possibility for macro capacities that can handle the exponentially rising number of devices in the fifth generation evolution and IoT era. Neural networks and deep learning techniques were adaptively applied to rapidly detect the fault locations and optimize the performance of these hybrid networks.

When it comes to prototyping methodically reciprocating systems and state-of-the-art alternatives, this is where system-on-chip (SOC) technology takes place. The vast need for executing multiple and highly diverting instructions calls for hugely integrated platforms specialized in various processing techniques and distinct architectures, including microcontrollers, digital signal processors, and reliable GPUs [19]. In recent years, the FPGA development pace has come up with a lot of chip families designers can pick from depending on the specifications required for the purposed application [19].

The key parameter of choosing the right processing aider is the milestone of the desired application. Compatibility of the processor used with the design specifications and future modification is crucial for picking the right tool. It is difficult to find the right hardware accelerator for a given application. There are many different types of digital signal processors (DSPs), FPGAs, and graphical processing units (GPUs), and the technical distinctions between them make it hard to compare them. Although they have different built-in architectures and software interfaces, they are capable of providing design platforms. The trade-offs between one type and another are the metric of comparison. Table 2 shows the pros and cons of using different processors.

Table 2. DSPs vs. FPGAs vs. GPUs [20].

Trade-Offs	DSPs	FPGAs	GPUs
Advantages	Sequential Algorithm Support.	Parallel and Reconfigurable Nature with high data throughput.	Instrumentation Projects Support and video processing support
	Low Developing Cost and free license	Moderate ownership cost	Low Cost
	Short Developing Time for Image Processing Algorithms.	High Energy Efficiency and Harsh Working Conditions Flexibility.	High Performance with Only Parallel Processing
Disadvantages	Not Suitable for High-Data Throughput Apps and incompatible with Parallel Algorithms.	Need for Technical Skills to Develop Reliable Designs and Long Development Time.	High Power Consumption.

For algorithms with high computing needs on a portable PC-independent device, FPGAs are the ideal alternative. For IBs to effectively communicate, a standalone established system that has a portable nature and dynamic capability is the optimal feature a smart network should have. FPGAs are low-power devices that may be employed in embedded systems. Instead of having separate circuitry designs that can merely cause noise and delay accumulations, resulting in falsified outputs, FPGAs help assemble the whole system in one stage [4,5]. Unlike other signal processing kits, FPGAs have high versatility in dealing with complex data types such as video streams, giving them the advantage of being a more reliable system hosting platform, enabling renovation and upgrading of the design to fit the most recent optimization requirements.

Different kinds of modulation are used according to the targeted data rate and the application hosting the system. There are a variety of techniques for modulating the source data into the EM wave carrier at any frequency range, including higher-level Intensity Modulation (IM) and On-Off Keying (OOK).

In [21], an indoor FPGA-based FSO communication system was developed using an 808 nm Infra-Red (IR) 100 mW laser source in which a Zedboard comprising the Xilinx XC7Z020-1CLG484C Zynq-7000 All Programmable System on Chip (AP SoC) associated with dual cortex ARM A9 processors. A data rate of 115 kbps was accomplished at a distance of 12 m via On-Off Keying (OOK) modulation to transmit text and audio files.

In this paper, an FPGA-based FSO system is used to transfer data at a distance of 12 m at a data rate of 115 kbps via basic OOK and an optimum bit rate of 230 kbps using IM/PWM is represented using an ALTERA Cyclone IV DE2115 Board with a pre-installed RISC-V software processor and a 650 nm Visible Light (VL) 5 mW laser source. The paper is divided into four further sections. Section 2 illustrates the idea of the implemented system. Section 3 clarifies the implementation steps that have been carried out on both software and hardware scales. Section 4 discusses the results obtained and, finally, the conclusion in Section 5 summarizes the work done.

2. Materials and Methods

The proposed system has the computer placed as the data server. The FPGA is directly linked with each computer via a universal asynchronous receiver transmitter (UART). This interface implies the usage of a serial communication technique in which the data is sent into the FPGA for processing and modulation. Reduced Instruction Set Computer Five (RISC-V) is installed into the FPGA for managing the sent data. The modulated data is streamed from the FPGA, as shown in Figure 2, to the laser driver circuit at the transmitting terminal, where the signal is amplified and converted from an electrical signal to an optical one. The red laser source was selected as the transmitting module due to its low cost, adaptability, and high data rates endurance. Focally concentrated beams that can travel

long distances are also one of its landmarks, thus it is a gradable versatile light source. The channel is conceptually a free space line of sight (LOS) medium.
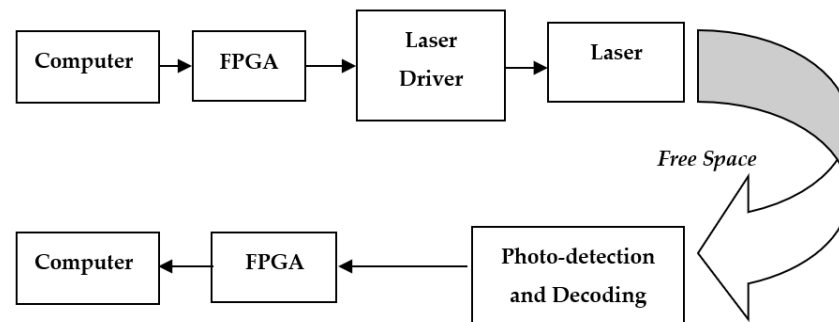

Figure 2. System Block Diagram.

Modulation schemes are one of the key factors that affect the performance of a communication system, given that the major drawback an FSO link can suffer from is a bad weather channel condition. Attenuation jeopardizing the quality of the received signal is the main driver of the transmitter specifications, including transmission configuration and the modulation scheme used. Originally, OOK is the simplest form a signal is modulated by where only one bit is sent in each clock cycle, where digital 1 is represented by full illumination, while digital 0 is represented when the laser is off [22]. The OOK is frequently plagued by spectral and energy efficiency issues. This sort of modulation approach also has amplitude distortion as a disadvantage. One way to overcome the drawbacks of OOK is using other modulation techniques such as Pulse Width Modulation (PWM) and Pulse Phase Modulation (PPM), where the amplitude interpretation is eliminated in the signal detection. Another "optical compatible" modulation technique that has shown a favored performance in the FSO system is IM. In IM, information is retrieved at the receiver side by detecting the intensity of received light, which is modulated as an information-carrying signal. Opposite to RF conventional communication that may include complex types of data, intensity-modulated signals are rather positive and real-valued [23]. Besides bypassing the OOK disadvantages, its simplicity and low-cost installation are other advantages of the IM technique. Reconfigurable algorithms can be established to pick the optimum modulation technique according to the type of data, transmission distance, and channel model. In this research, the implemented system initiated a study that compares the realization of OOK and IM schemes in terms of data rate since these two modulation schemes are the most commonly used in FSO implementations, and the fact that IM can be integrated with other modulation techniques that control the light intensity makes it an interesting approach for further optimization and modification. Higher-level IM, on the contrary, uses a single clock cycle to transmit more than one bit depending on the number of levels that power would be divided into. The power ratio then encodes the bit symbol into a certain voltage level that controls the illumination of the laser beam. Here, this is done by controlling the pulse width of the output transmitting power.

A mapping algorithm is completed using MATLAB to compare the frequencies of the incoming data. As shown in Figure 3, if the frequency happens to be less than or equal to 115 kHz, OOK is used. Otherwise, IM is the chosen technique. Thus, the most suitable modulation is configured for reliable communication with less power consumption. Figure 4 shows how bandpass filters (BPF) can filter out random data ranges to determine the desired modulation used. These BPFs can be adjusted according to any further desired data frequency ranges. The FPGA was the kit of target due to being a compatible environment in which hardware building and reconfiguration is a fast process with easy modification availability. It also enables designers to create a bottom-up implementation of any hardware system prototype, ensuring that the final product is bug-free.
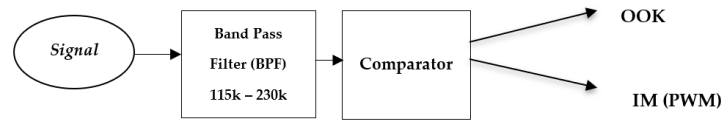
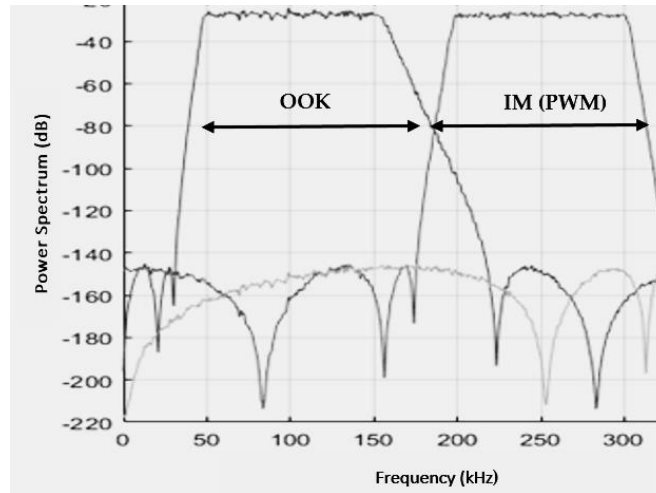**Figure 3.** Mapping Algorithm Block Diagram.

Figure 4. Rough Power and Frequency Data Filtering according to their frequency band.

Channel Model

The received signal model in wireless communication systems is generally represented in (1).

$$r(t) = x(t) \otimes h(t) + n(t) \tag{1}$$

In which

- x(t) is the original signal;
- h(t) is the channel effect function;
- and n(t) is the summed-up noise.

The total received signal is the resulting combination between the original signal x(t) convoluted with the channel effect function h(t) and additional noise n(t) summed up in the transmission. That noise is mostly implicating light surroundings, thermal noise, shot noise, and dark currents that are modeled as Additive White Gaussian Noise (AWGN). The encountering interferences and jamming threats upon RF signals are eliminated due to the high immunity of optical signals.

One of the key installation parameters FSO links are prone to consider is the angle of transmission. For rooftop applications requiring LOS frequent availability, the light beam emission angle must be aligned with the receiver position at a horizontal (180°) angle with a slight acceptable error of ±5° about the photo-detector area collecting the optical signal [24]. This gives total power (in watts) emitted from a uniform source, as represented in (2).

$$P_T = BA_S\Omega_S \tag{2}$$

In which

- P_T is the total transmission power;
- B is the brightness function;
- A_S is the surface area;
- and Ω_S is the emission angle.

The above equations are valid for any free space communication link performance analysis. With the aid of a converging lens, the light from the source beam can be concentrated on a single point to reduce attenuation levels and scattering losses. For the used laser source, a focal lens is adopted to focus the output optical signal. The source has an

aperture of 12 mm in a dot shape. The module is set perpendicular to the mirror interface at 90° so that the silicon-based photo-detector of 7.5 mm^2 and sensitivity angle $\varphi = \pm 65°$. For fixed transmission angle, sensitivity angle, and receiving surface area, the brightness becomes a function of the total transmission power.

3. Implementation

This section is divided into two parts: software and hardware. The software part of the system is encapsulated in the processing done on the ALTERA FPGA Cyclone IV DE2-115 board that has a RISC-V processor software version installed for input data management. RISC-V is an open specification platform that allows designers to use open-source cores, utilized at low power mode, unlike ARM, Intel, and AMD processors, which need licensed products, owned IP, and use complex instruction set computer (CISC) technique, hence, they have high power consumption. Newly intriguing computing methodologies and integrating engineering applications acquire the presence of robust simulation and testing kits that can stimulate the process of innovation in both software and model-ware forms, which are capable of supporting and validating the design flow. Model-ware, often known as Model-Driven Development (MDD), is a broad area that supports a variety of technologies by increasing software development productivity. With highly defined software isolation domains that are continuously up to date, developers can frequently upgrade their designs and ensure the security of data [25]. It is highly used for multimedia applications and file compressions, thus an optimum processing option for the proposed design.

The communication between the FPGA and the computer is obtained via a Universal Asynchronous Receiver Transmitter (UART) RS232 cable for transmission and a Universal Serial Bus (USB) for the reception. The proper modulation technique is selected according to the required data rate and mapped to be performed by the software interface (Quartus Prime 18.0) of the FPGA. Higher-level Intensity Modulation (IM) was the item of choice, controlling the illumination of the laser beam accordingly. Four power levels were given as the constellations of data required to be transmitted. The levels were represented as 0%, 33%, 66%, and 100% of the power. Tera Term and Putty user interfaces were used to test the data sent in a text form, while MATLAB was the test bench used for audio data.

The modulated signal is fed from the FPGA General Purpose Input Output (GPIO) into a laser driver circuit where it is amplified using a common emitter configuration amplifier manifesting the selection of a TIP31C power transistor that boosts the transmission into a 650 nm Visible Light (VL) red laser source. The FPGA input signal is directed to the base of the transistor while the output signal is taken from the collector to the laser source, as shown in Figure 5. The emitter is connected to a 3.3 V supply.
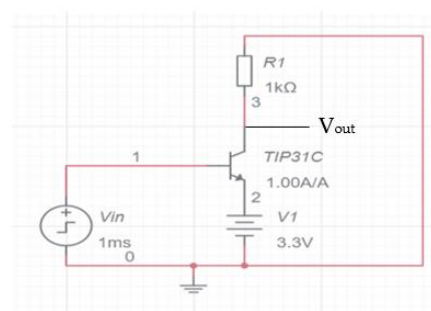

Figure 5. Laser Driver Circuit.

If the o/p of a collection of circuits linked as a system reaches a fixed value in a finite time, it is said to be stable. A system is considered to be unstable if its o/p rises with time rather than stabilizing. Multiple ways are used to determine the stability of a circuit. For BJT stability, the rate of change of collector current with respect to the reverse saturation current can be the metric of stability measurement. The maximum collector-base voltage in saturation mode is 1.2 V at a collector current $I_C = 3$ A, while the transit frequency for

current gain is f_T = 3 MHz at I_C = 500 mA [26]. The operating margin for the BJT is ensured, and a consistent current flows via R1 and is supplied into the laser module since the circuit is run in low power mode, with V1 continually 3.3 V plugged out of the DC port on the FPGA board and Vin dependent on the set character voltages from the PC. Hence, the input current to the laser module is constantly stabilized in the range of milli Ampere.

The optimal transistor was chosen based on the power amplifying specifications required to transfer the optical signal at the greatest possible distance. After experimentations, the application of the TIP31C transistor became apparent. When considering power amplification abilities and the fact that the optical signal required a highly powered-up gain to traverse the requisite distance between the transmitter and the receiver, there was a significant performance enhancement.

A mirror reflects the laser beam at half the distance (D/2) back to the photo-detector to achieve a distance D of 12 m between the transmitter and the receiver. The existence of the mirror was used to verify the system's compatibility in outdoor settings between adherent buildings or in the design of multipath signals employing smart building mirror glazed architecture. Double the setup distance is achieved by practically inducing the mirror to reflect the signal at half the distance D/2. Figure 6 shows the practical system setup for complete hardware testing. The use of building walls as transmission points between one another with the concept of numerous signal reflections is emphasized by the fact that smart buildings present the idea of glazed exterior layers. Hence, adapting multi-node FSO networks can be installed.
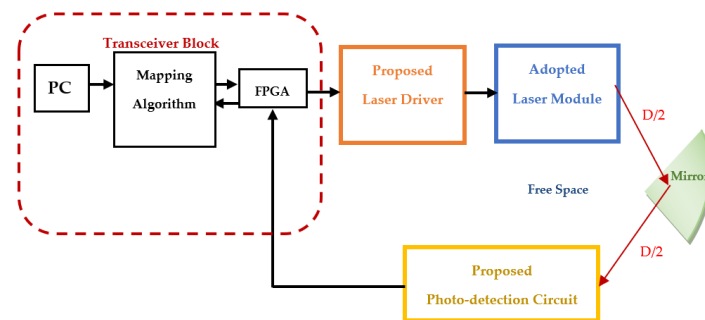

Figure 6. Proposed System Setup.

Figure 7 shows the schematic and amplification of a 100 mV input signal via a common emitter amplifier circuit using TIP31C. The output voltage has shown an increase to around 270 mV amplitude with the use of the TIP31C transistor, as shown in Figure 8. Figure 9 also shows the o/p collector current against time for the given sample circuit. This has demonstrated the dependability of using the TIP31C transistor as the driver and photo-detection circuit's building block. It was also demonstrated in the hardware deployment that the increase in gain allowed the optical signal to be more illuminated and travel the required distance.
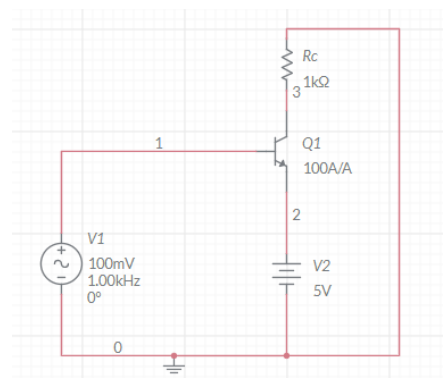

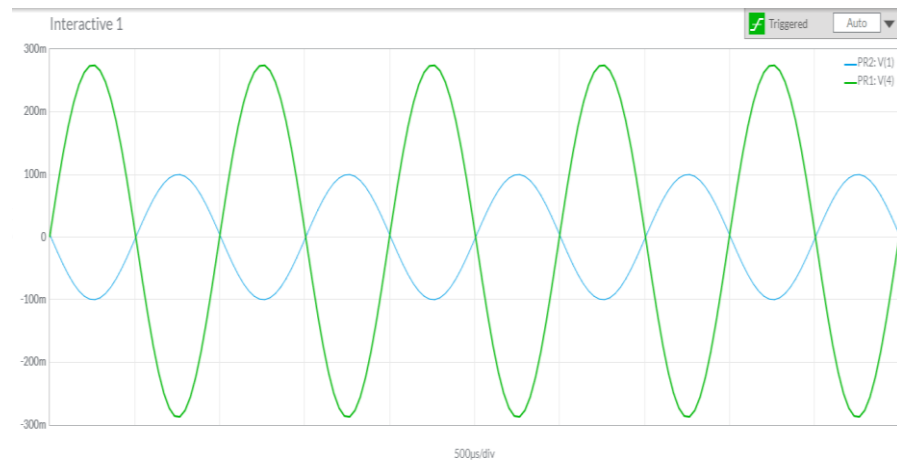**Figure 7.** Initial testing driver circuit for TIP31C.

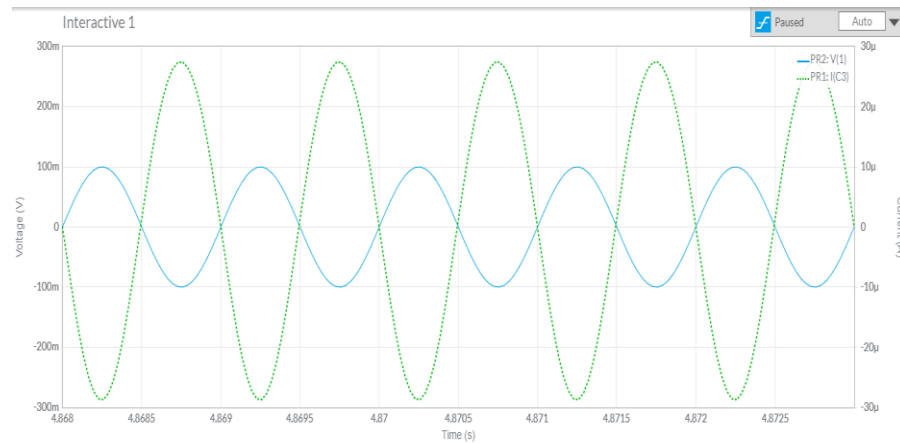**Figure 8.** Output Voltage Signal for TIP31C Transistor.

Figure 9. Output Current Signal for TIP31C Transistor.

The power levels were properly adjusted to meet the targeted four laser intensities in the VHDL part, as shown in Table 3, using a trial testing of the amplitude of the voltage for optimum detection of the received bits. The levels are initialized in a hexadecimal form. Figure 10 shows the simulation results on ModelSim. The pulse width of the waveform represents the percentage of power for each illumination level.

Table 3. PWM Levels.

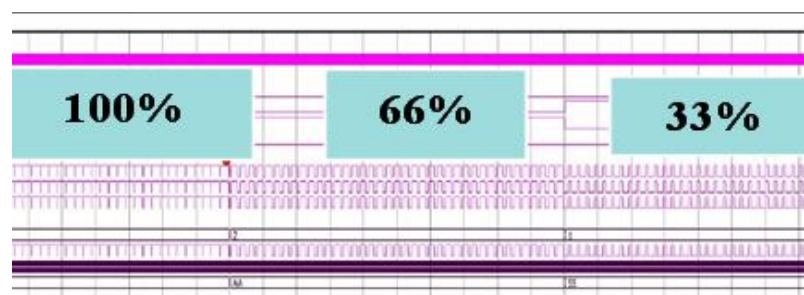| Amplitude Level in Hexadecimal	Power Percentage
00	0%
65	33%
72	66%
FF	100%

Figure 10. ModelSim Simulation Waveform.

The laser light intensity varies along with the distinction of the data being transmitted, and the beam is carried in free space from the transmitting to the receiving point. At the receiver terminal, the BPW34 Photodetector catches the optical signal where it is reverted to an electrical one. BPW34 is a silicon-based high sensitivity photodiode packaged in a plastic capsule with a water-clear epoxy surface texture. It can detect visible and infrared radiations. Its detecting area is considered relatively high (A = 7.5 mm^2) with a wide varying viewing angle ($\varphi_s = \pm 65°$). The reverted electrical signal is then passed to a comparative Analog to Digital Conversion (ADC) demodulating circuit, as shown in Figure 11, to interpret the four voltage levels into logical ones to be read by the receiver USB port from the FPGA into the computer via the GPIO input pin. The circuit is constructed using the concept of the differential pairing of TIP31C BJT. Here, a combination of four comparative differential pairs is used to measure the difference between the reference voltage and input laser voltage for a maximum value of 3.7 V. If the input voltage is greater than the reference voltage, the output voltage will be 3.7 V (Logic "1"), as shown in Figure 12. There are four reference voltages for each comparator so the output will be divided into four logical levels according to the input analog voltage.
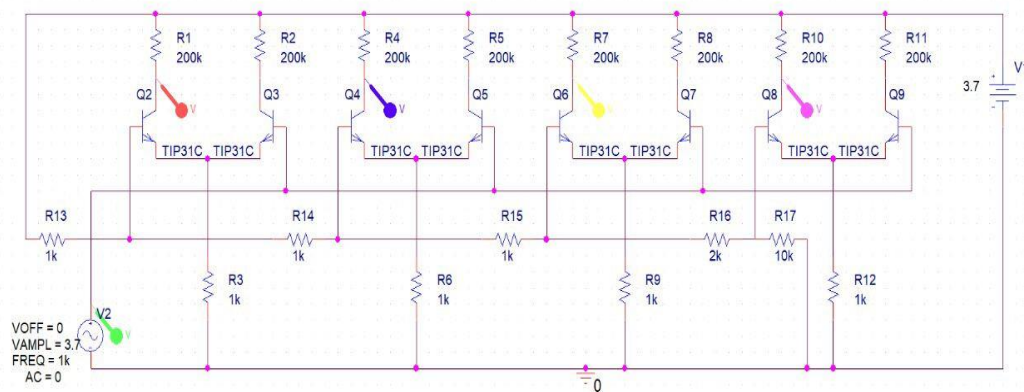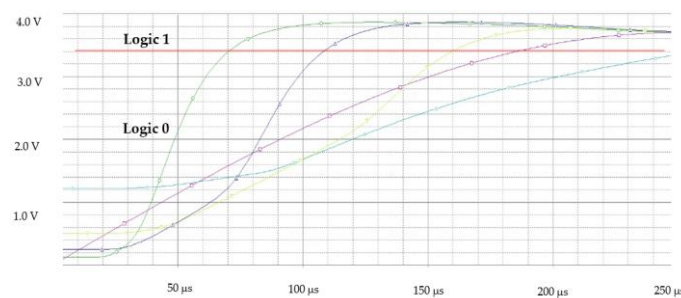

Figure 11. Demodulation Circuit.

Figure 12. Simulation Output.

The components used to build up the proposed system are listed in Table 4.

Table 4. Components Properties.

Component	Type Used
FPGA	ALTERA Cyclone IV DE2-115
Processor	RISC-V Software Processor
Programmable Logic	VHDL
Optical Source	650 nm 5 mW VR Laser
Amplifying Transistor	TIP31C
Photo Detector	BPW34

Figure 13 shows a flowchart intensifying the algorithmic approach accomplished by the system, stating logically how data flows from the transmitting to the receiving point.
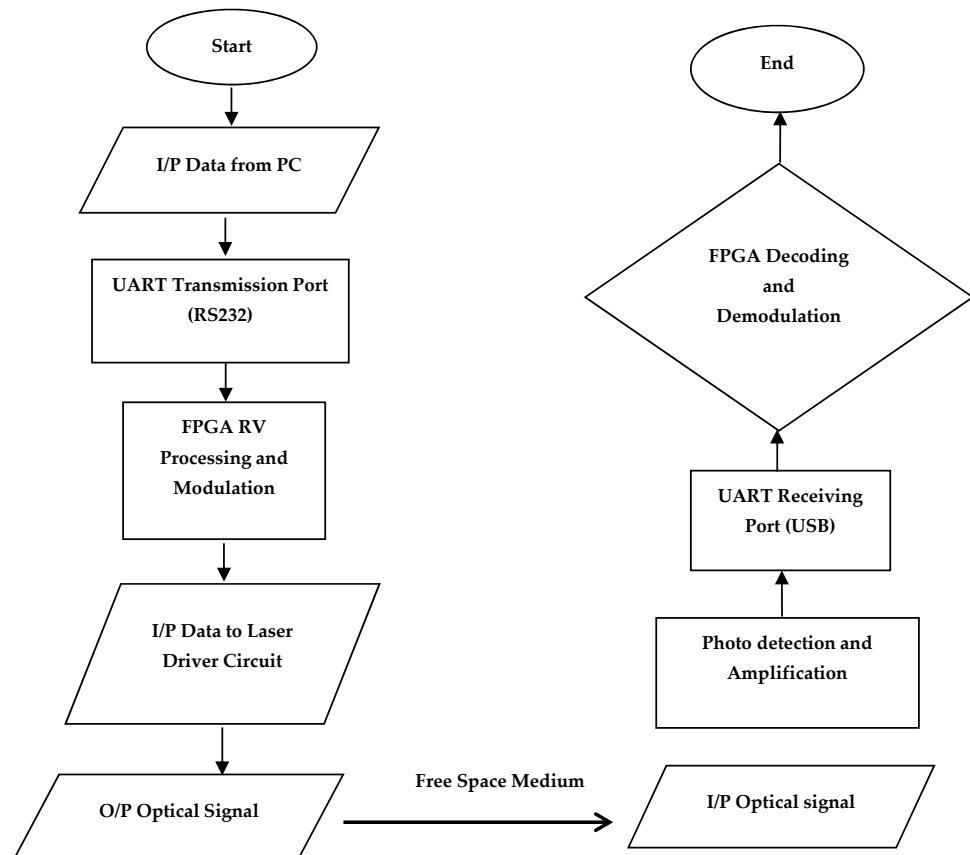

Figure 13. System Flowchart.

4. Results

The experimentation has been staged to test each part of the system individually. First of all, the UART communication between FPGA and the PC via the application of the RISC-V processor data management technique was tested before indulging the laser communication part into the system. The laser module used had a 5 mW maximum power. Second of all, the optical communication line was fully tested using the OOK modulation technique at a reached data rate of 115 kbps and a distance of 12 m. Lastly, the IM/PWM technique was applied in the Quartus software interface controlling the illumination of the laser module to achieve a doubled data rate of around 230 kbps. Initially, Figure 14 shows the UART successful half-duplex channel between the PC and FPGA with the additional processing help of RISC-V via Linux Mint interface before including the hardware optical system components.
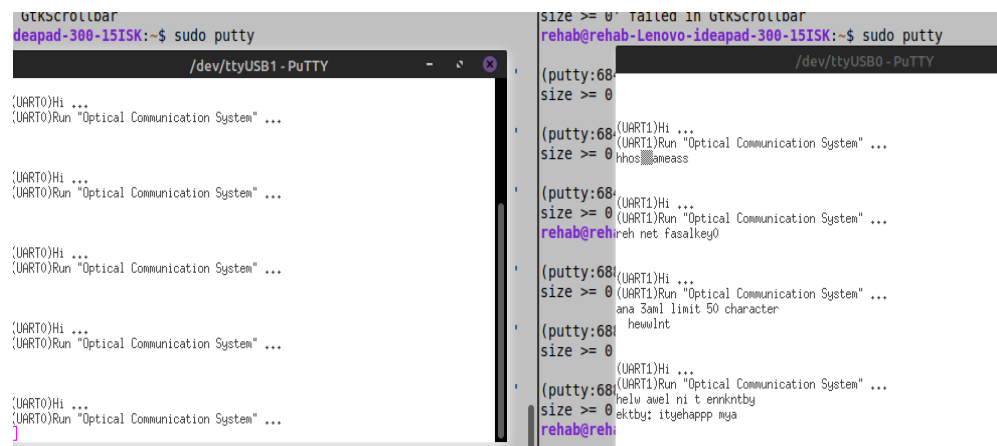
Figure 14. UART random text Communication between FPGA and PC.

4.1. Software Results

The simulation of the receiver circuit was tested for different optical input signal voltages to validate the recognition of bit levels based on the power constellation division done at the modulation stage. For both the laser driver and photo-detection circuit, the TIP31C transistor was the most compatible chip with the desired specifications due to its high switching capability and power utility, making it frequently used in power linear applications and various amplifying stages. Figure 15 shows the output voltages at each comparator terminal represented in the left collector voltages of each transistor for a fed 3.7 V optical signal. The threshold voltage for logic high detection was designed in the proposed circuit to be 3 V, while any less value will be received as logic low. Hence, the four transistors will be on, and their output voltages are interpreted to be logic high.
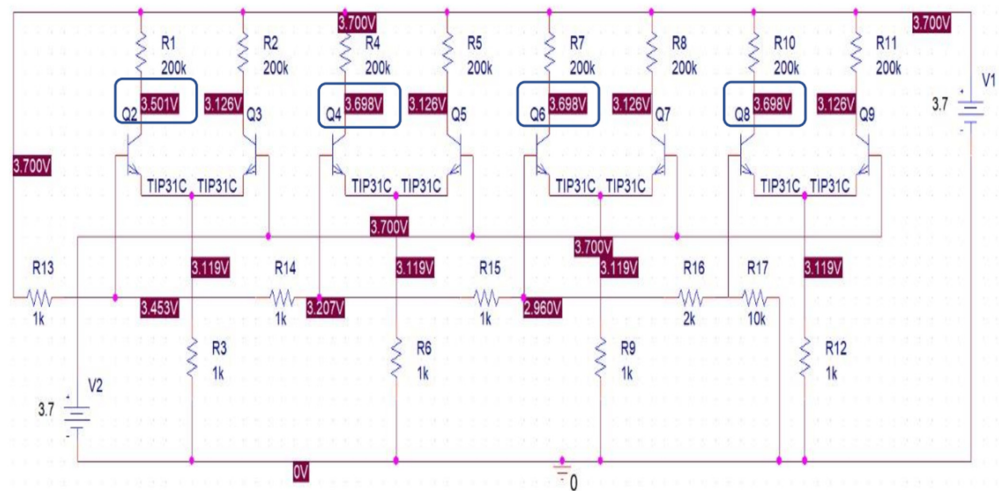

Figure 15. Receiver Circuit Simulation for 3.7 V input.

Another example is shown in Figure 16, where the input optical signal voltage is 2 V. The output at Q6 and Q8 is high, while Q4 and Q2 had their collector voltages lowered, resulting in a logic low recognition. This can be summed up as four logic combinations depending on the bit constellation received by the photo-detector.
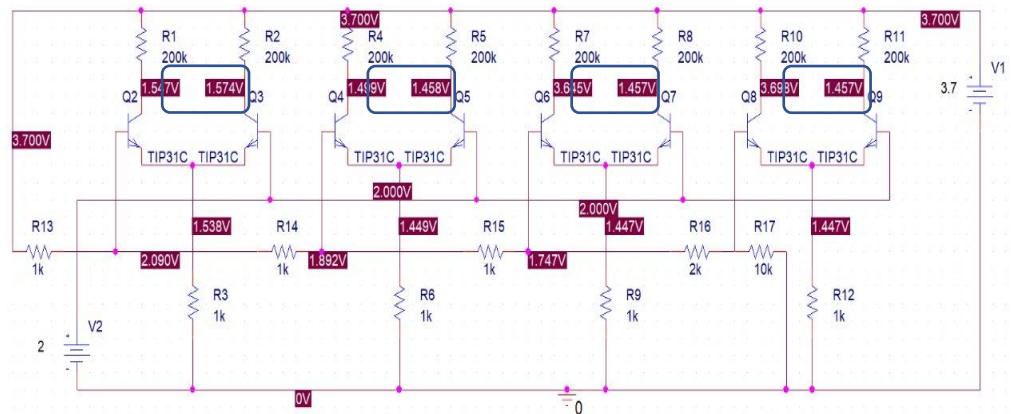
Figure 16. Receiver Circuit Simulation for 2 V input.

4.2. Hardware Results

Figure 17 shows the ALTERA Cyclone IV DE2115 board used for the proposed design with the transmitting and receiving UART cables. The RS232 and USB ports were tested as two independent lines for transmission and reception, respectively, on Linux Mint OS using PUTTY.
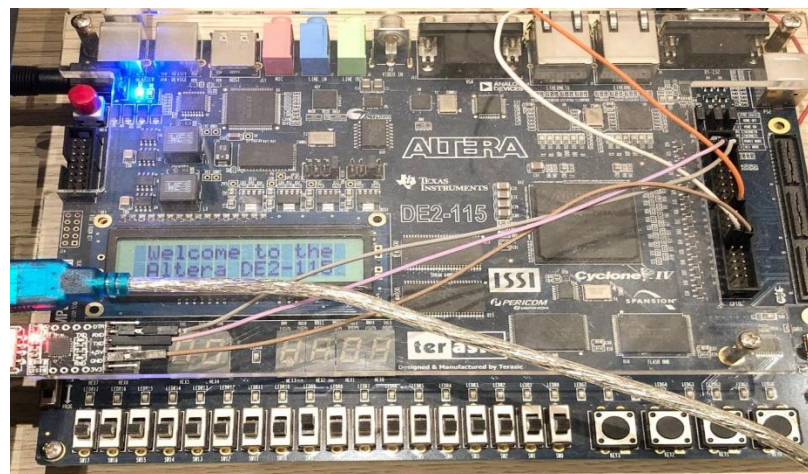

Figure 17. The ALTERA FPGA Kit of the proposed system.

To test the communication system, using one FPGA kit as a transceiver, the laser beam was directed to the mirror that reflects it to the photo-detecting circuit. Figure 18 shows the hardware implementation of the system in the darkness to avoid any external lighting interference during transmission. This can further frame this design into a capsulated ASIC implementation in an opaque box to mitigate any lighting interference that could degrade the communication performance.
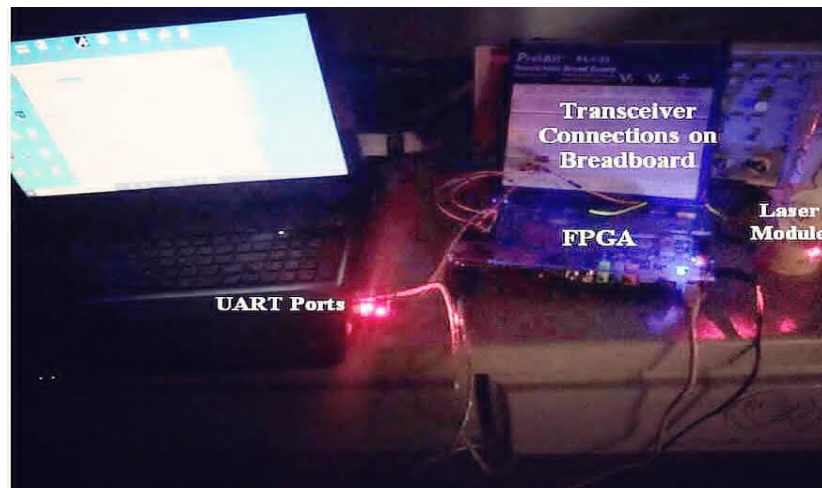
Figure 18. Transceiver Hardware System Implementation.

With the optimized modulation scheme, a data rate of approximately 230 kbps is obtained, as shown in Figure 19. The received signal is then detected and demodulated using a comparator threshold decision circuit to correctly decode the incoming bits and interpret them to their original form. Figure 20 shows the incoming characters' successful reading.

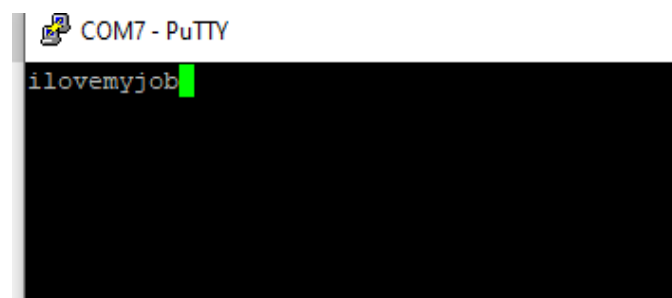**Figure 19.** The achieved data rate of the proposed system.

Figure 20. Text Characters successfully received at the UART reception port.

The photo-detection circuit design has an amplifying comparative approach that determines the threshold voltage required for demodulation. For audio transmission, MATLAB was the test bench where a predefined file space was used to capture the data sent. The size of the file was monitored along with a message detecting the number of errors in the received bits for each transmission.

4.3. Power Budget

Establishing the low power feature of the proposed system, power calculations have been performed to validate the aspect. Starting with the FPGA processing part, the total power dissipated from the FPGA processing and modulation stage was analyzed, as shown in Table 5.

Table 5. FPGA Power Consumption Summary.

Summary	Power Consumed
Core Dynamic Thermal Power Dissipation	1.56 mW
Core Static Thermal Power Dissipation	98.54 mW
I/O Thermal Power Dissipation	59.51 mW
Total Thermal Power Dissipation	159.61 mW

The maximum output power from the second transmitting stage comprising the laser driver circuit was 5 mW operating at around 16 mA, alternating downwards with the intensity modulation level required for each bit symbol transfer. At the receiving end, the photo-detection and demodulation circuit is powered up using a 3.7 V supply initiated to drive the BPW34 photo-sensor and the comparators needed to convert the received signal and decode it. For '11' bit symbol recognition, the optical signal power will be 100% reciprocating as 3.3 V powering the four comparing stages, which is the maximum power of the electrically reverted signal.

The quality of the constructed communication link can be measured according to multiple parameters affecting the communication channel and internal infrastructure of the setu Here, all parameters will be summed up in a metric constant k that equals one, excluding the two hyper values that are monitored to evaluate the system: the data rate and total power consumed. This figure of merit can be summed up as shown in (3).

$$G = k\frac{R_B}{P_T} \tag{3}$$

In which

- G is the figure of merit;
- k is the metric constant;
- R_B is the received bit rate;
- and P_T is the total power of the system.

Since the optimal reached data rate of the proposed system is 115 kbps for OOK and 230 kbps for the IM/PWM technique, the power budget and the figure of merit can be calculated for both techniques. For OOK and output power of around 165 mW, the figure of merit can be written as (4). For IM/PWM and input power of around 180 mW, the figure of merit is calculated in (5).

$$G = \frac{115 \times 10^3}{165 \times 10^{-3}} = 698 \times 10^3 \text{ b/sW} \tag{4}$$

$$G = \frac{230 \times 10^3}{180 \times 10^{-3}} = 1.28 \times 10^3 \text{ b/sW} \tag{5}$$

A remarkable note is that the figure of merit G represents a qualitative measurement of the communication system. As it increases, this would imply either a leap in the received data bits, which indicates an improved reception rate, or a decrease in the total power of the system, which indicates more energy efficiency. Figure 21 shows how an enhanced data rate improves the figure of merit at a constant overall system power, while Figure 22 shows that as the total power increases, the figure of merit decreases due to lowered efficiency at a fixed data rate.
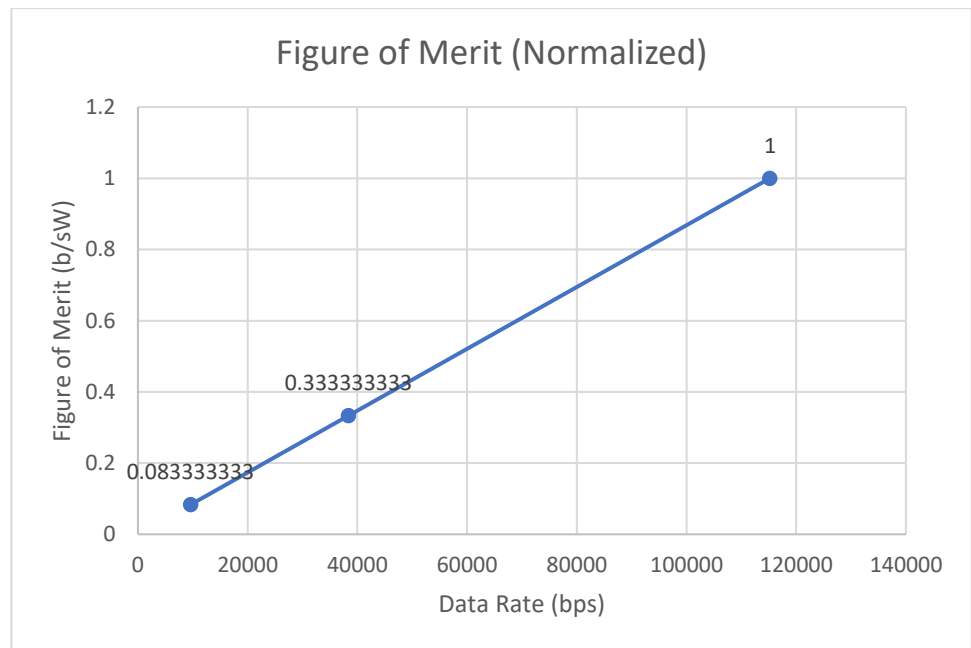
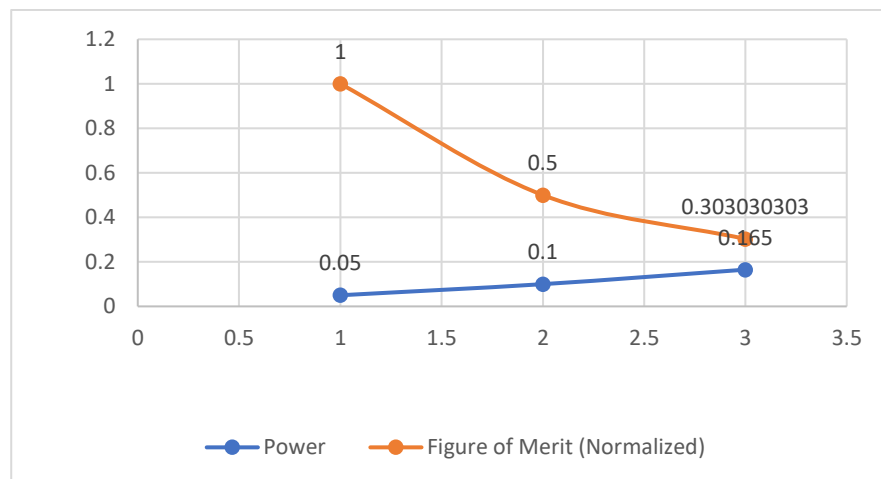**Figure 21.** Figure of Merit against data rate at fixed total power.

Figure 22. Figure of Merit (b/sW) change with power (W) at a fixed data rate.

5. Discussion

Given the laser source specifications and the tested distance between the transmitter and the receiver, a quality metric of the data rate is compared via two kinds of modulation, OOK and IM/PWM technique, and a pre-defined figure of merit is declared and calculated for each scenario. The IM approach achieves a doubled data rate of 230 kbps by dividing the power into 4 separate modulated levels. As a result, instead of the OOK modulation with logic '1' as the on state and logic '0' as the off state, the constellations now have 4 potential combinations: '00', '01', '10', and '11'. Another remarkable advantage of IM modulation is its simplicity. It does not require complex interpretation or extra hardware components. It also has a huge versatility to be integrated with any other kind of modulation based on the desired platform and type of communication application. However, forward error correction methods can be applied to the transmitted signal to enhance the quality of detection of the proposed system. A qualitative approach is done in terms of the data rate and total consumed power of the system combined in the evaluated figure of merit 'G' that represents the improved performance of the system as its value increases due to either

bettered data rate or lowered power consumption. This has been illustrated using a plotted graph for each parameter vs. the normalized values of G. Adaptive theory is also one of the future milestones, in which multiple modulation techniques can be embedded and the optimization algorithm can pick the most suitable modulation according to the required data type (text, audio, or video) and rate to be sent. Hence, a fully functioning monitoring communication spot is obtained between smart buildings.

6. Conclusions

This paper illustrates a prototype low-power FPGA-based wireless optical communication system for building-to-building communication utilizing the advantages of license-free FSO technology. LOS communication at a distance of 12 m and data rate of 115 kbps via OOK and 230 kbps via higher-level IM was successfully implemented for various types of data, including text and audio files. A 650 nm 5 mW laser module was used for transmission. A measurement of the system quality was analyzed using a figure of merit that is purely a function of the received data rate and total power used. It was confirmed and proven that by lowering power consumption and increasing the received data rate, an optimum figure of merit and higher system performance can be achieved. Higher data rates can be obtained using the proposed system with advanced light sources as well as extended distance records for much further range outdoor applications. Adaptive algorithms can also be developed for more modulation technique optimization, and the system can be enhanced using artificial intelligence models that would help pre-analyze the system conditions and channel estimation models to reinforce its performance. Using versatile FPGA boards as a base design platform is a robust election in altering the specifications of the system to meet new technological challenges and further modification techniques.

Author Contributions: R.A.: Methodology, Investigation, System Analysis and Implementation, Writing—Original Draft, and Visualization. H.E.: Software Installment and Simulation Analysis. H.H.A.: Investigation, Supervision, Writing Review, Editing, and Validation of Implementation. S.M.E.: Conceptualization of the FPGA part of the project, Supervision, Writing Review, and Editing. M.A.: Conceptualization of the FSO part of the project, supervision, Writing Review, and Editing. All authors have read and agreed to the published version of the manuscript.

Institutional Review Board Statement: Not applicable.

Informed Consent Statement: Not applicable.

Data Availability Statement: Not applicable.

References

1. Sánchez-Corcuera, R.; Nuñez-Marcos, A.; Sesma-Solance, J.; Bilbao-Jayo, A.; Mulero, R.; Zulaika, U.; Azkune, G.; Almeida, A. Smart cities survey: Technologies, application domains and challenges for the cities of the future. *Int. J. Distrib. Sens. Netw.* **2019**, *15*, 155014771985398. [CrossRef]
2. Tan, S.Y.; Taeihagh, A. Smart city governance in developing countries: A systematic literature review. *Sustainability* **2020**, *12*, 899. [CrossRef]
3. Brad, B.; Murar, M. Smart Buildings Using IoT Technologies. *Stroit. Unikal'nyh Zdanij I Sooruz. Constr. Unique Build. Struct.* **2014**, *5*, 15. Available online: http://search.proquest.com/docview/1559660128/ (accessed on 1 March 2022).
4. Garg, A.K.; Janyani, V.; Batagelj, B.; Abidin, N.H.Z.; Bakar, M.H.A. Hybrid FSO/fiber optic link based reliable & energy efficient WDM optical network architecture. *Opt. Fiber Technol.* **2021**, *61*, 102422. [CrossRef]
5. Kaushal, H.; Kaddoum, G. Optical Communication in Space: Challenges and Mitigation Techniques. *IEEE Commun. Surv. Tutor.* **2017**, *19*, 57–96. [CrossRef]
6. Tawfik, M.M.; Sree, M.F.A.; Abaza, M.; Ghouz, H.H.M. Performance Analysis and Evaluation of Inter-Satellite Optical Wireless Communication System (IsOWC) from GEO to LEO at Range 45000 km. *IEEE Photonics J.* **2021**, *13*, 7301006. [CrossRef]
7. Marbel, R.; Yozevitch, R.; Grinshpoun, T.; Ben-Moshe, B. Dynamic Network Formation for FSO Satellite Communication. *Appl. Sci.* **2022**, *12*, 738. [CrossRef]

8. Mansour, A.; Mesleh, R.; Abaza, M. New challenges in wireless and free space optical communications. *Opt. Lasers Eng.* **2016**, *89*, 95–108. [CrossRef]

9. Georlette, V.; Moeyaert, V.; Bette, S.; Point, N. Outdoor Optical Wireless Communication: Potentials, standardization and challenges for Smart Cities. In Proceedings of the 2020 29th Wireless and Optical Communications Conference (WOCC), Newark, NJ, USA, 1–2 May 2020. [CrossRef]

10. Zhu, X.; Kahn, J.M. Free-space optical communication through atmospheric turbulence channels. *IEEE Trans. Commun.* **2002**, *50*, 1293–1300. [CrossRef]

11. Khalighi, M.A.; Uysal, M. Survey on free space optical communication: A communication theory perspective. *IEEE Commun. Surv. Tutorials* **2014**, *16*, 2231–2258. [CrossRef]

12. Sharma, S.S.D.; Khan, S.A. Literature Survey and issue on Free Space Optical Communication System. *Int. J. Eng. Res. Technol.* **2015**, *4*, 561–567. Available online: www.ijert.org (accessed on 1 March 2022).

13. HajiRassouliha, A.; Taberner, A.J.; Nash, M.P.; Nielsen, P.M.F. Suitability of recent hardware accelerators (DSPs, FPGAs, and GPUs) for computer vision and image processing algorithms. *Signal Process. Image Commun.* **2018**, *68*, 101–119. [CrossRef]

14. Malik, A.; Singh, P. Free Space Optics: Current Applications and Future Challenges. *Int. J. Opt.* **2015**, *2015*, 945483. [CrossRef]

15. Sadiku, M.N.O.; Musa, S.M.; Nelatury, S.R. Free Space Optical Communications: An Overview. *Eur. Sci. J.* **2016**, *12*, 55. [CrossRef]

16. al Safi, A.; Bazuin, B. Toward digital transmitters with Amplitude Shift Keying and Quadrature Amplitude Modulators implementation examples. In Proceedings of the 2017 IEEE 7th Annual Computing and Communication Workshop and Conference (CCWC), Las Vegas, NV, USA, 9–11 January 2017. [CrossRef]

17. Coding, B.M. LED Visible light communication system based on FPGA. *IEEE Trans. Commun.* **2015**.

18. Haq, A.F.M.S.; Yuksel, M. Multi-element full-duplex FSO transceiver design using optimum tiling. *Opt. Commun.* **2021**, *501*, 127377. [CrossRef]

19. Yang, H.; Wang, B.; Yao, Q.; Yu, A.; Zhang, J. Efficient Hybrid Multi-Faults Location Based on Hopfield Neural Network in 5G Coexisting Radio and Optical Wireless Networks. *IEEE Trans. Cogn. Commun. Netw.* **2019**, *5*, 1218–1228. [CrossRef]

20. Andina, J.J.R.; de la Torre Arnanz, E.; Peña, M.D.V. *Advanced Signal Processing Resources in FPGAs*; Routledge: London, UK, 2017. [CrossRef]

21. Sarkar, T.S.; Sinha, B.; Mukherjee, S.; Joardar, I.; Mazumdar, S. Development of an FPGA based Indoor Free Space Optical (FSO) Communication System using 808 nm Infrared (IR) LASER Source. In Proceedings of the 2020 IEEE Calcutta Conference (CALCON), Kolkata, India, 28–29 February 2020; pp. 313–317. [CrossRef]

22. Miglani, R.; Charak, S.; Arora, S.K.; Masud, M. A Review On FSO By Using Different Modulation Techniques. *Int. J. Eng. Technol.* **2018**, *7*, 136. [CrossRef]

23. Chaaban, A.; Rezki, Z.; Alouini, M.S. On the Capacity of Intensity-Modulation Direct-Detection Gaussian Optical Wireless Communication Channels: A Tutorial. *IEEE Commun. Surv. Tutor.* **2022**, *24*, 455–491. [CrossRef]

24. Majumdar, A.K. Chapter 8—Free-Space Optical Communications: Role and Integration With the Internet of Things. *Opt. Wirel. Commun. Broadband Glob. Internet Connect.* **2019**, 245–258. [CrossRef]

25. Martin-Diaz, I.; Moriñigo-Sotelo, D.; Duque-Perez, O.; Romero-Troncoso, R.D.J. Advances in Classifier Evaluation: Novel Insights for an Electric Data-Driven Motor Diagnosis. *IEEE Access* **2016**, *4*, 7028–7038. [CrossRef]

26. Available online: https://www.alldatasheet.com/ (accessed on 21 April 2022).